

Parameterization of Ice Growth for Numerical Calculations of Cloud Dynamics

L. RANDALL KOENIG—*The Rand Corporation, Santa Monica, Calif.*

ABSTRACT—Parametric equations describing the growth of ice particles in the range 10^{-11} – 1 g are presented. Three subranges (10^{-11} – 5×10^{-8} , 5×10^{-8} – 10^{-4} , and 10^{-4} – 1 g) are used. The parametric equations were developed with the aid of a complex method of calculating ice-particle growth. Two approaches to using the parametric equations in a simulation resembling a natural cloud situation are described. One method breaks the ice-particle spectrum

into three components, the sizes of each being monitored. The other assumes a size distribution that can be characterized by a "growth-median" size, so that only one size need be monitored to describe the rate of growth. The parametric method is compared with more complicated methods in a simulated cloud environment, and the results are regarded as satisfactory.

1. INTRODUCTION

This work was initiated because of a desire to include microphysical effects in a numerical model predicting the life cycle of cumulus clouds (Murray 1970). The cloud model used is based on thermo-hydrodynamic equations of motion. Since the microphysical and cloud scales are quite dissimilar, it was judged impractical to formulate detailed descriptions of the physics of both within a single model. Therefore, a search was initiated for means to parameterize microphysical phenomena. Kessler (1967, 1969) has developed a useful method of parameterizing liquid-phase microphysical events. The goal of the present work was to develop a means to parameterize ice-phase phenomena in a manner comparable to and compatible with Kessler's formulation.

Two processes are of primary concern: (1) diffusion of water vapor to and away from ice particles and (2) accretion of liquid drops on ice particles. Ice-phase aggregation was ignored, both on the basis of its assumed minor role in the clouds (cumuli) of interest and because there is little information to calibrate the parameterization of that process.

2. METHODOLOGY

Predicting the growth of ice particles is complicated because of their many shapes, bulk densities, and fall speeds—even for particles of a given mass. Growth may occur by either diffusion or agglutination, or both. Diffusion predominates during the early period of growth and, if liquid droplets are plentiful, agglutination is dominant after moderate sizes are achieved.

To devise parametric procedures for computing the rate of growth of ice particles, one needs reference rates of growth as functions of crystal size, temperature, and liquid-water content. The primary source of our data was a numerical simulation that has been compared with observation, at least insofar as diffusion is concerned.

As a standard of reference, a series of growth predictions was prepared using a relatively complex method of calculating ice-crystal growth by diffusion (Koenig 1971b) that was augmented by a method of computing the collection of water droplets. The simulation of riming was necessarily crude, for there are few data concerning this process with which the accuracy of the model could be compared. Observations suggest that there is a minimum size below which ice crystals do not collect water droplets. It is not clear that this threshold is real; that is, that the flow field around the ice particle excludes contact with the droplets. Quite likely, it is only an apparent threshold resulting from collection rates that are low relative to vapor-phase growth at small sizes. If there is a true threshold, it must be a function of crystal shape, bulk density, fall speed, and so forth. In any event, a riming threshold was used to facilitate parameterization. A threshold of $100 \mu\text{m}$ in maximum dimension, independent of crystal habit, was assumed.

The mass of rime acquired by an ice particle was assumed equal to the liquid water density times the volume of the column of air equivalent to the product of the area of the ice crystal measured perpendicular to its direction of fall and the difference in fall distance between ice and liquid particles. Riming was assumed uniform over the entire surface of the crystal; in accordance with this assumption, as riming became predominant, the crystal's shape became less eccentric and in time nearly spherical. The bulk density increased, approaching 0.8 as riming continued. Crystal fall velocity was computed as a fraction of the fall velocity of a drop of equal mass. The fraction used increased with proportion of riming, ranging from that appropriate to the crystal type to 0.7.

The desire for accuracy of the empirical growth equations must be balanced by the need for their simplicity and for rapidity of computation. On the basis of inspection of the series of computations using the complex model, it was decided to divide ice-particle growth into three zones.

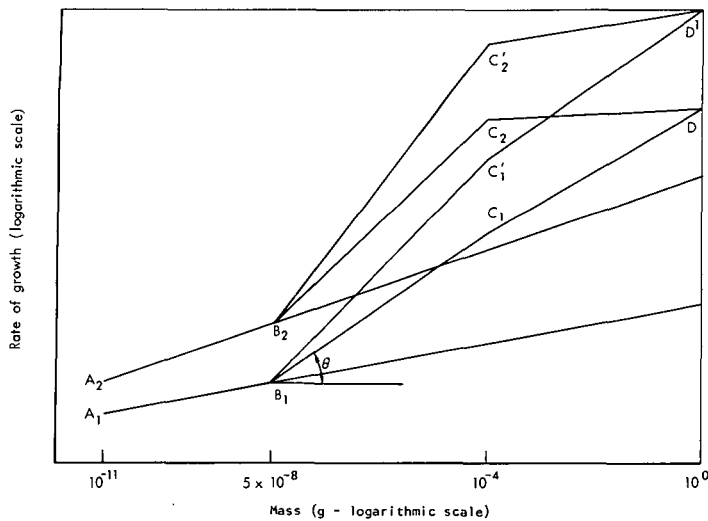


FIGURE 1.—Illustration of the concept of parameterization. Growth at constant temperature and liquid-water content follows path ABCD. Subscripts indicate growth properties at different temperatures; primed and unprimed points indicate growth properties at different liquid-water contents.

TABLE 1.—Symbols used in this paper

a_1, a_2	diffusion growth parameters (temperature sensitive)
b_1, b_2	growth parameters (liquid-water-content sensitive)
f	growth rate multiplying factor
m	mass (g)
m_c	growth median mass of ice particle (g)
q	water vapor mixing ratio
q_{sl}	water vapor mixing ratio at liquid saturation
q_{si}	water vapor mixing ratio at ice saturation
t	time (s)
C_i	constant
D_c	volume-median diameter of ice particle (m)
N	ice-particle concentration (number \cdot m $^{-3}$)
N_0	ice concentration at zero mass intercept on presumed Marshall-Palmer distribution
T	temperature ($^{\circ}$ C)
ρ_i	ice content (bulk density) (g \cdot m $^{-3}$)
ρ_l	liquid-water content (bulk density) (g \cdot m $^{-3}$)

In the first, only diffusion occurs, and growth rate is solely a function of temperature (liquid saturation is assumed). In the second, both diffusion and riming occur, and in the third, only riming occurs. If there is less than 0.05g \cdot m $^{-3}$ of liquid water present in the cloud, diffusion only is assumed in all zones. Figure 1 illustrates the concept of the parameterization. Crystals are assumed initially to have a mass of 10 $^{-11}$ g. Their growth rate follows an exponential dependence on mass; that is,

$$\left. \frac{dm}{dt} \right|_{A \rightarrow B} = a_1(m)^{a_2} \quad (\text{g/s}) \quad (1)$$

The symbols used in this paper are given in table 1.

The parameters a_1 and a_2 are temperature dependent and are adjusted so that the segment AB approximates

TABLE 2.—Values of parameters a_1 and a_2 as functions of temperature*

Temperature ($^{\circ}$ C)	a_1	a_2
0	0	0
−1	0.7939(−7)	0.4006
−2	.7841(−6)	.4831
−3	.3369(−5)	.5320
−4	.4336(−5)	.5307
−5	.5285(−5)	.5319
−6	.3728(−5)	.5249
−7	.1852(−5)	.4888
−8	.2991(−6)	.3894
−9	.4248(−6)	.4047
−10	.7434(−6)	.4318
−11	.1812(−5)	.4771
−12	.4394(−5)	.5183
−13	.9145(−5)	.5463
−14	.1725(−6)	.5651
−15	.3348(−4)	.5813
−16	.1725(−4)	.5655
−17	.9175(−5)	.5478
−18	.4412(−5)	.5203
−19	.2252(−5)	.4906
−20	.9115(−6)	.4447
−21	.4876(−6)	.4126
−22	.3473(−6)	.3960
−23	.4758(−6)	.4149
−24	.6306(−6)	.4320
−25	.8573(−2)	.4506
−26	.7868(−6)	.4483
−27	.7192(−6)	.4460
−28	.6513(−6)	.4433
−29	.5956(−6)	.4413
−30	.5333(−6)	.4382
−31	.4834(−6)	.4361

*In the a_1 values, the exponent of 10 is shown in parentheses (e.g., 0.7939(−7) = 0.7939 \cdot 10 $^{-7}$).

the growth behavior of a crystal growing by diffusion (Fig. 1 contains two members, representing growth at two different temperatures, of the family of segment AB.) The extension of segment AB represents growth rate versus mass for diffusive growth only, at all masses. The parameters a_1 and a_2 are given in table 2. They are derived from a least-squares fit to the model of growth by diffusion (Koenig 1971b). The point B signals the end of growth by diffusion only. Observations suggest a dimensional criterion for establishing point B as was used in the complex computations, but the necessary compromises have resulted in a mass criterion. By changing the position of point B, one can achieve greater accuracy in certain temperature or liquid-content ranges (at the expense of other regions). In this study, the crystal mass at point B is uniformly 5 \times 10 $^{-8}$ g; the growth rate can be determined from eq (1) using the appropriate parameters for a_1 and a_2 . In the region BC, growth rate is a function of both temperature and liquid-water content. Growth rate as a function of mass is assumed to follow BC until the mass of the particle is 10 $^{-4}$ g. The tangent of the angle θ

between BC and the horizontal from B is determined from the liquid-water content. By definition,

$$\tan \theta = \frac{\ln \left(\frac{dm}{dt} \right) - \ln \left(\frac{dm}{dt} \right)_{m=5 \times 10^{-8}}}{\ln(m) - \ln(5 \times 10^{-8})}. \quad (2)$$

By empirical fit,

$$\tan \theta = 1 + \frac{\ln \rho_l}{10}. \quad (3)$$

The numerical constants in eq (3) were derived from an inspection of plots of growth rate versus liquid-water content for various temperatures and a choice of values of θ that favors the warmer regions of ice-crystal growth (0 to -10°C). The point B in figure 1 is determined by eq (1), using a mass of 5×10^{-8} and values of a_1 and a_2 appropriate to the ambient temperature. Hence in the region BC, the growth rate is computed by

$$\left. \frac{dm}{dt} \right|_{B \rightarrow C} = a_1 (5 \times 10^{-8})^{a_2} \left(\frac{m}{5 \times 10^{-8}} \right)^{\tan \theta} \quad (\text{g/s}). \quad (4)$$

The ratio of the maximum to minimum dimension of an ice particle decreases, and the bulk density increases as it becomes larger and riming predominates. Eventually, the particle assumes a spherical shape. Hence, particles tend toward uniformity, and the growth rate of a particle of given mass is dependent solely upon the liquid-water content. This effect is simulated by making the growth rate (g/s) equal to ρ_l ($\text{g} \cdot \text{m}^{-3}$) divided by 1000 when the particle reaches a mass of 1 g (point D). The transition from C to D is assumed to follow a straight line in figure 1. Hence,

$$\left. \frac{dm}{dt} \right|_{C \rightarrow D} = b_1 \left(\frac{m}{10^{-4}} \right)^{b_2} \quad (\text{g/s}) \quad (5)$$

where

$$b_1 = a_1 (5 \times 10^{-8})^{a_2} (2000^{\tan \theta}) \quad (6)$$

and

$$b_2 = \frac{\ln \left(\frac{10^{-3} \rho_l}{b_1} \right)}{\ln(10^4)} \quad (7)$$

The parameters a_1 and a_2 are those appropriate to the ambient temperature (given in table 2). They are the only empirical, variable quantities used in the parameterization that are not quantities either of the particle (e.g., mass) or of the environment (e.g., ρ_l). If temperature and liquid-water content are held constant, the growth-rate curve will consist of straight lines, as illustrated in figure 1. In general, however, as growth occurs, temperature and liquid-water content change, and the curves of growth rate versus mass will not describe straight lines.

The level of complexity of these equations precludes accurate simulation of ice-particle growth in all ambient conditions found in clouds. Consequently, in assigning values for constants that appear in the equations, either one can strive for a more or less uniform goodness-of-fit throughout the range of conditions of interest or one can

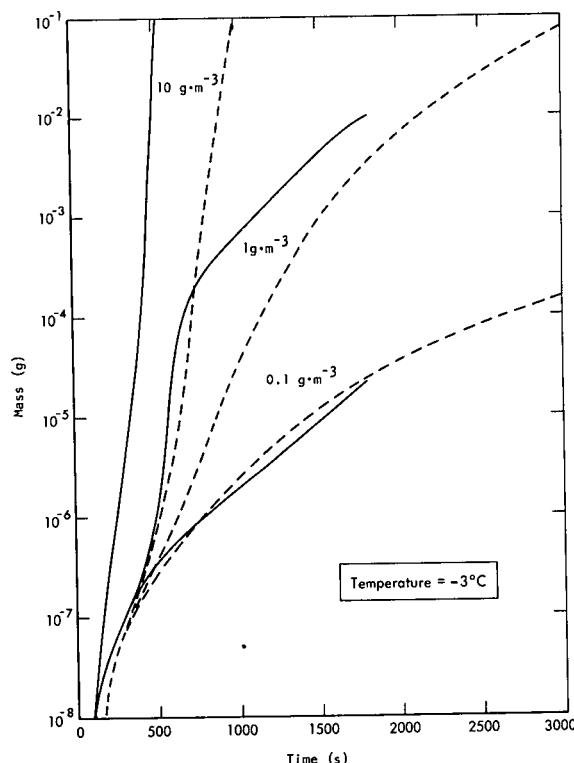


FIGURE 2.—Comparison of the growth histories of individual ice particles at -3°C for various liquid-water contents, as predicted by the complex (solid lines) and parametric (dashed lines) schemes.

tailor the fit to conditions believed to be of particular importance, to the detriment of fit to other conditions of lesser importance. The mass at point B, where dependence on liquid-water content begins, and the dependence of the angle θ on liquid-water content are two of the most important factors that can be manipulated.

3. RESULTS

Figures 2–4 show sample comparisons between computations of the growth of a single particle using the parametric equations developed in the previous section and those using the complex methods of calculating ice growth based on the diffusion model proposed by Koenig (1971b) with riming added. Comparison calculations were made at 1°C intervals to -20°C . Liquid-water content and temperature are constant in each of these calculations. Time steps of 10 s in an Eulerian integration scheme were used with the parametric method. The goodness-of-fit is a function of temperature and liquid-water content. In all cases, at high liquid-water content, the mass predictions of the parametric scheme lag those of the complex method. At more typical water contents, values from the parametric scheme may lag or lead, depending upon temperature; not uncommonly, the growth curves intersect. The predicted mass of an ice particle after a given growth period may be quite accurate, but more commonly it is in considerable error. The percentage

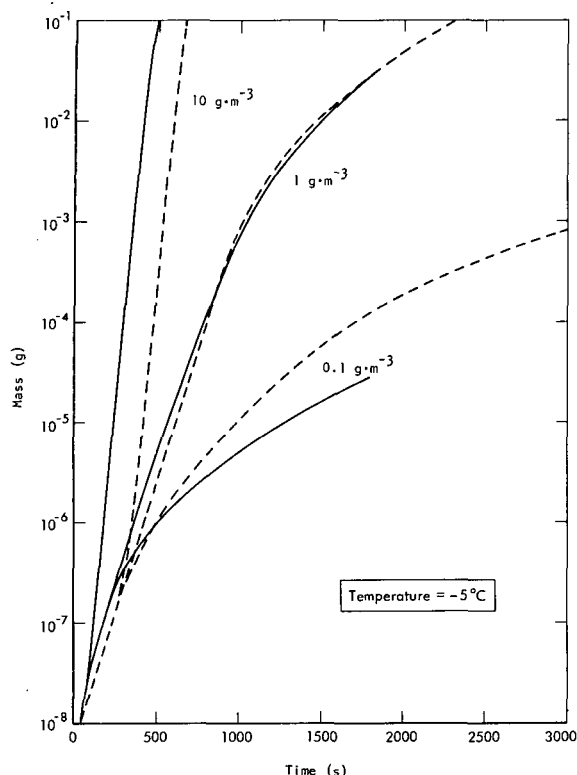


FIGURE 3.—Same as figure 2 except at -5°C .

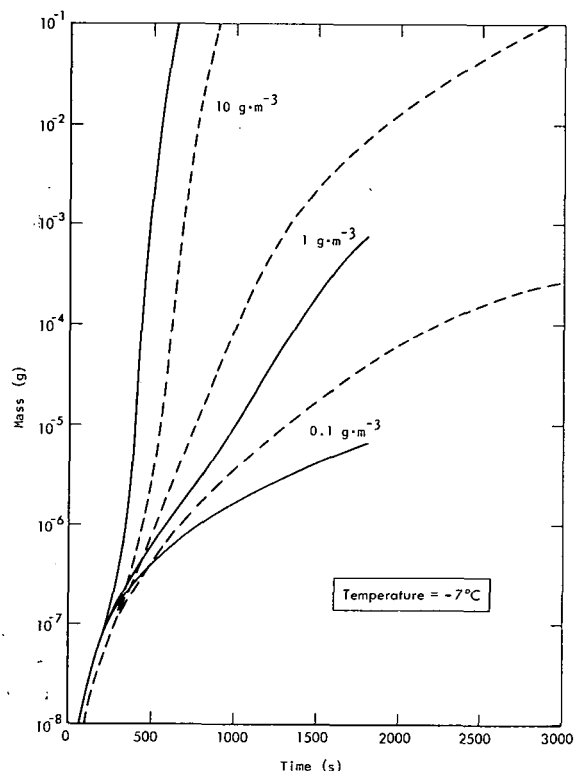


FIGURE 4.—Same as figure 2 except at -7°C .

error in the predicted period of time required to achieve a given mass is generally less than the percentage error in predicted mass after a given time increment. Also, as shown in Koenig (1971b), the parameterization closely

duplicates the complex calculations at zero liquid-water content.

For the purposes for which this parameterization was made, it is most appropriate to examine the characteristics and to judge the utility of the scheme in predicting the liquid-ice metamorphosis in situations resembling a cloud; that is, in an environment in which temperature, liquid-water content, and ice-crystal concentration fluctuate. This was done by preparing a simple program in which temperature and condensed water were linear functions of an assigned draft velocity. Values of temperature and condensed water approximated that of a moist adiabat. Condensed water was partitioned between liquid and ice, with changes in the ice content being determined by the concentration of ice particles and their growth rates. The concentration of ice crystals as a function of temperature followed an exponential curve, increasing by one order of magnitude with each temperature drop of 4°C . The concentration is given by

$$N = \frac{C_i}{10^{(T/4)}} \quad (\text{m}^{-3}) \quad (8)$$

where T is temperature in degrees Celsius and C_i is a constant (equal to unity for "natural" ice-crystal concentrations).

One of the problems that arises in parameterizing ice-particle growth is that of describing the size-distribution spectrum. Early experimentation showed that in situations where temperature decreased with time (as in a rising cumulus tower), the concentration of ice particles increased at a rate similar to the rate of growth. If all particles are assumed identical, then the mass of each particle is the total bulk density of ice divided by concentration, and because of increasing numbers of ice particles, the assumed mass of individual particles remains too small; consequently, growth rates are too low and time required for glaciation too long. To circumvent this problem, it is necessary to provide some description of an ice-size spectrum. Two methods were devised.

One method divides the ice spectrum into at most three groups: crystals nucleated (1) between 0° and -5°C , (2) between -5° and -10°C , and (3) at temperatures between -10° and -15°C . All the crystals in a given group are identical in size. Thus, if the temperature of the cloud remains warmer than -5°C , only one category of ice is used. If the temperature decreases from the 0° to -5°C region to fall within -5° to -10°C , one category comprises the number of crystals nucleated in the region 0° to -5°C (which remains fixed in number concentration but grows in ice bulk density). A second category comprises crystals nucleated in the -5° to -10°C range, N in number, as given in eq (8), minus the concentration in the 0° to -5°C category [in which N is given by setting $T = -5^{\circ}\text{C}$ in eq (8)]. Similar considerations apply for temperatures in the range -10° to -15°C . If the temperature falls below -15°C , a new category (-15° to -20°C) is created; but to maintain only three categories, the 0° to -5°C and -5° to -10°C categories are combined, the concentration and total mass being the sum of the

original categories. Similar considerations apply if the temperature falls below -20°C . Gravitational separation has not been incorporated into the parametric models used in this work, but in a model under construction, particles of one category falling into a warmer temperature region lose their identity but have their mass added to that of the category proper for the temperature.

A second method we developed to account for the ice-particle spectrum is more analogous to Kessler's (1969) parameterization of the liquid state. In this case, ice particles are assumed to have a density of $0.7\text{ g}\cdot\text{cm}^{-3}$ and to follow a Marshall-Palmer type of distribution, with the total concentration of ice particles varying with temperature in accordance with eq (8). Following Kessler's (1969) formulation [using his equations (8.4), (8.5), and (8.10)], we obtain the zero intercept

$$N_0 = \left(\frac{38.51 \times N}{\rho_i^{1/4}} \right)^{4/3} \quad (\text{m}^{-4}) \quad (9)$$

and the volume-median diameter is

$$D_v = 0.0953 \left(\frac{\rho_i}{N_0} \right)^{1/4} \quad (\text{m}). \quad (10)$$

We define a "growth-median" mass (m_g) as the mass of a particle whose incremental growth multiplied by the total number of ice crystals present equals the total incremental growth of the ice-particle spectrum. Thus,

$$m_g = \frac{\int_{i=0}^{i=\infty} N_i dm}{N} \quad (\text{g}). \quad (11)$$

Through trial and error experimentation, m_g was related to the volume-median diameter in accordance with

$$m_g = \frac{\pi}{6 \times 10^6} [0.4483 D_v]^3 \quad (\text{g}). \quad (12)$$

The growth-median mass was used to determine the rate of growth using the system of eq (1)–(7). The volume-median diameter would be used in calculating gravitational separation.

Computations simulated the rise of a cloud mass above the 0°C level, and an initial liquid-water content (simulating condensation at temperatures higher than 0°C) was assumed. The vertical-rise rate was held constant and gravitational separation was not taken into account.

Because no suitable observational data are available, a more complex cloud model containing simulations of condensation, diffusion, and riming was used as the criterion of the ability of the scheme to predict occurrences in nature. Condensation, vapor-ice diffusion, and ambient temperature, water vapor, density, and so forth were simulated using rather complex procedures (Koenig 1968, 1971a, 1971b). Riming was simulated using the same procedures as in the previous calculations with constant temperature and constant liquid-water content. The vapor density and condensed-water content within the cloud volume were governed by the updraft and the rates of condensation and vapor-ice diffusion. Ice-crystal concen-

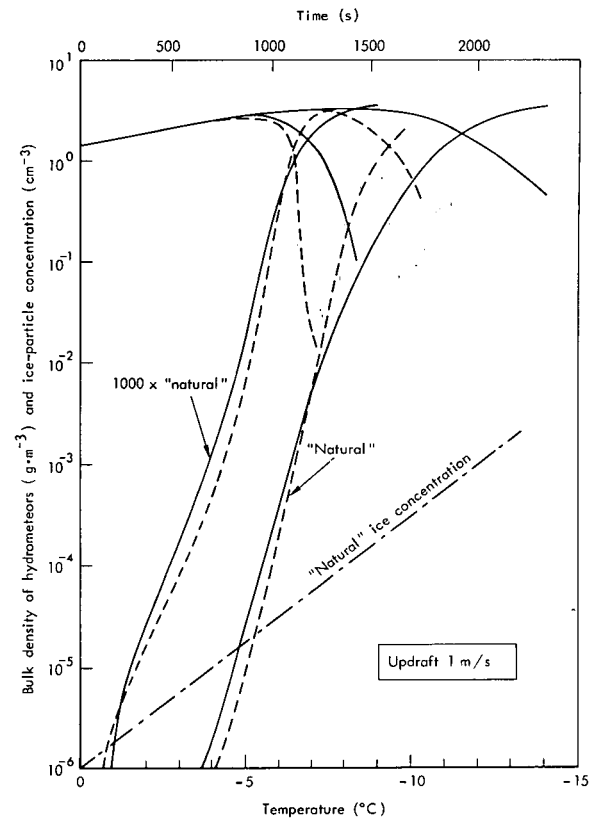


FIGURE 5.—Comparison of microphysical properties of a parcel rising 1 m/s, as predicted by the complex (solid lines) and the three-particle parametric (dashed lines) schemes. The steeply rising lines show ice content, the initially slowly rising lines show liquid content.

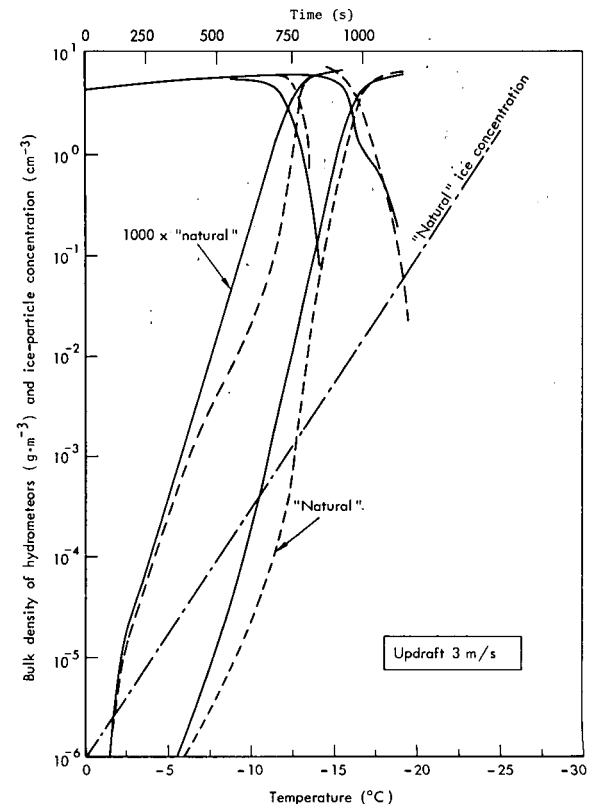


FIGURE 6.—Same as figure 5 except 3-m/s parcel rise.

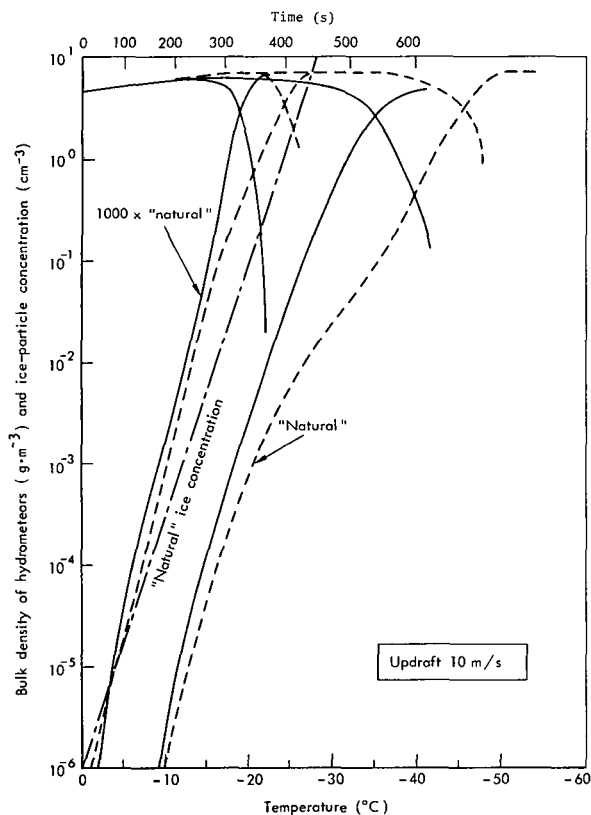


FIGURE 7.—Same as figure 5 except 10-m/s parcel rise.

trations followed the same equation used in the simple parametric model. We initially assumed a cloud-free, water-vapor-saturated parcel having a specified temperature and condensation nucleus content. As in the simple model, a specified updraft creates the cooling that leads to cloud formation; however, in the complex model, cooling follows the adiabatic lifting process with corrections for latent heats of phase changes. Sample comparisons of the results of the first parametric scheme (using three categories of ice particles) with the more complex "control" scheme are shown in figures 5–7. Sample comparisons of the results of the second parametric scheme (employing one size representing an assigned distribution) with those of the more complex control scheme are shown in figures 8–10.

Since the parametric model was "calibrated" using a model that automatically adjusted the water-vapor density for the local conditions that will affect this variable (primarily temperature, draft velocity, ice, and drop contents), no correction for the effects of vapor density on the growth rates is generally required. However, if simulation of a cloud containing only ice particles growing by diffusion is attempted (i.e., along AB extended in fig. 1) and the water-vapor mixing ratio is independently computed, an adjustment of the growth rate is indicated. A suggested form to compute f , a multiplying factor for the right side of eq (1), is

$$f = \frac{q_{st} - q_{st}}{q - q_{st}} \quad (13)$$

The value of this feature has not been examined, however.

It is important to model the rate of ice production so as to satisfactorily predict the rate of release of latent heats

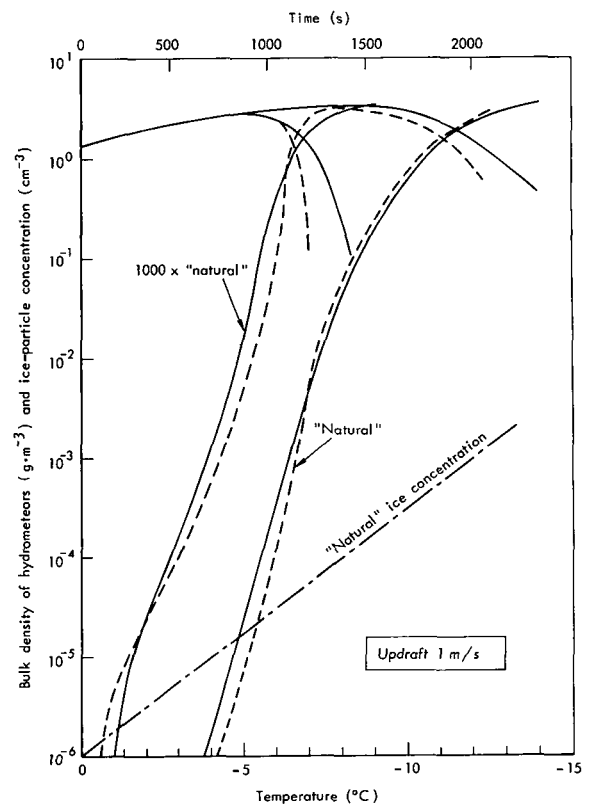


FIGURE 8.—Comparison of microphysical properties of a parcel rising 1 m/s, as predicted by the complex (solid lines) and the one-particle parametric (dashed lines) schemes. The steeply rising lines show ice content, the initially slowly rising lines show liquid content.

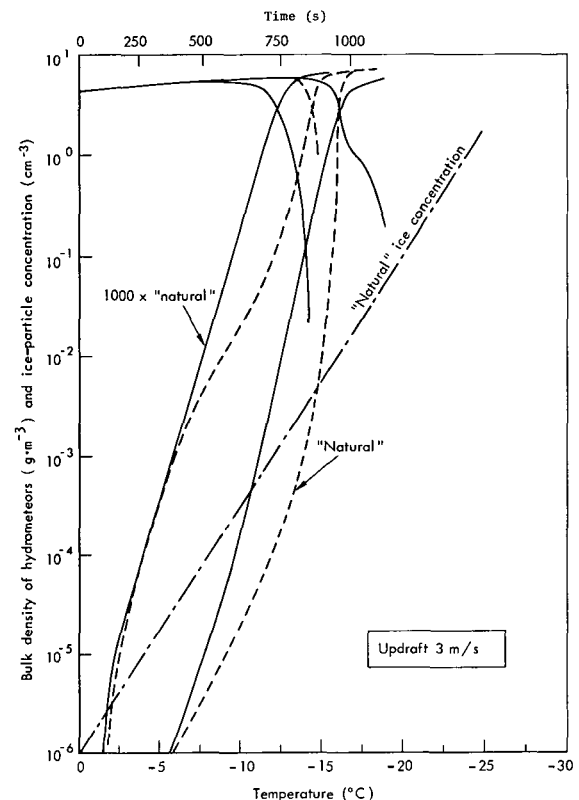


FIGURE 9.—Same as figure 8 except 3-m/s parcel rise.

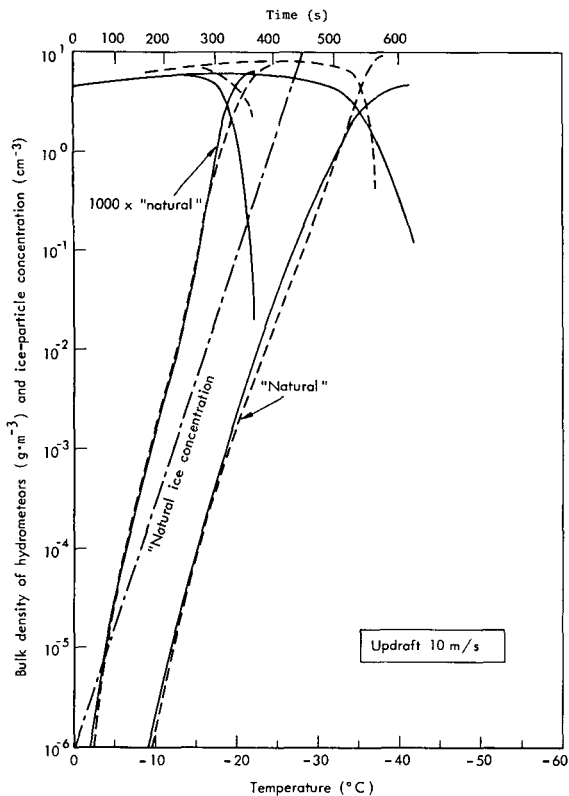


FIGURE 10.—Same as figure 8 except 10-m/s parcel rise.

of freezing and sublimation. Useful "one-value" comparisons are either the length of time required to convert the clouds to equal proportions of ice and liquid hydrometeors or the temperature at which this occurs. There is a relatively long induction period prior to this point, but once it is reached, glaciation proceeds rapidly. On the basis of these criteria, the tests reveal that the parametric models portray rather well the important features of cloud glaciation. The three-crystal method appears somewhat better at lower draft speeds, the one-crystal method, somewhat better at higher draft speed.

All three models predict the following features, which appear qualitatively correct (no quantitative data are available):

1. The rapidity of glaciation is a function of ice-crystal concentration; the more crystals, the faster the conversion.
2. The more rapid the updraft, the faster (in time) glaciation occurs, but the colder the cloud for a given amount of ice.
3. The shape of the conversion curve (mass of ice as a function of time) appears proper insofar as there appears to be an incubation period in which little ice is in evidence, followed by a short period in which rapid and essentially complete conversion of liquid to ice occurs.

The last characteristic, rapid conversion after a relatively long incubation period, suggests that temperature and draft-velocity criteria for conversion are useful for extremely simple parameterization. Figure 11 is intended to aid in the development of this form of parameterization. Given an updraft velocity and ice-nucleus concentration (expressed in terms of multiples of "natural"

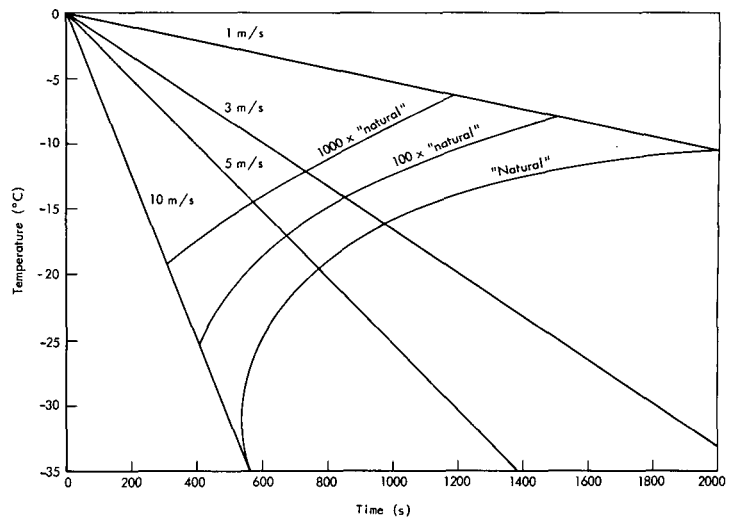


FIGURE 11.—Time/temperature summary for glaciation of clouds having various ice-particle contents and rates of rise.

concentration), one can find a time and temperature of conversion.

It should be emphasized that, throughout this paper, the term "natural ice concentration" refers to an ice concentration-temperature relationship expressed by eq (8) (and graphically shown in figs. 5–10). This relationship is somewhat arbitrary. For example, if natural ice multiplication is believed to occur, natural ice concentrations may be greater than those given by eq (8), and some modification of figure 11 would be proper to adjust the time-temperature relationship for glaciation.

ACKNOWLEDGMENT

This work was performed under the sponsorship of the Experimental Meteorology Laboratory of NOAA [Contract E22-17-71(N)]. The continual interest and support of Joanne Simpson in our cloud modeling efforts is sincerely appreciated.

REFERENCES

- Kessler, Edwin, "On the Continuity of Water Substance," *ESSA Technical Memorandum IERTM-NSSL 33*, U.S. Department of Commerce, National Severe Storms Laboratory, Norman, Okla., Apr. 1967, 125 pp.
- Kessler, Edwin, "On the Distribution and Continuity of Water Substance in Atmospheric Circulations," *Meteorological Monographs*, Vol. 10, No. 32, American Meteorological Society, Boston, Mass., Nov. 1969, 84 pp.
- Koenig, L. Randall, "Numerical Modeling of Condensation," *Research Memorandum RM-5553-NSF*, The Rand Corporation, Santa Monica, Calif., Aug. 1968, 43 pp.
- Koenig, L. Randall, "Numerical Experiments Pertaining to Warm-Fog Clearing," *Monthly Weather Review*, Vol. 99, No. 3, Mar. 1971a, pp. 227–241.
- Koenig, L. Randall, "Numerical Modeling of Ice Deposition," *Journal of the Atmospheric Sciences*, Vol. 28, No. 2, Mar. 1971b, pp. 226–237.
- Murray, Francis W., "Numerical Models of a Tropical Cumulus Cloud With Bilateral and Axial Symmetry," *Monthly Weather Review*, Vol. 98, No. 1, Jan. 1970, pp. 14–28.

[Received August 26, 1971; revised March 3, 1972]